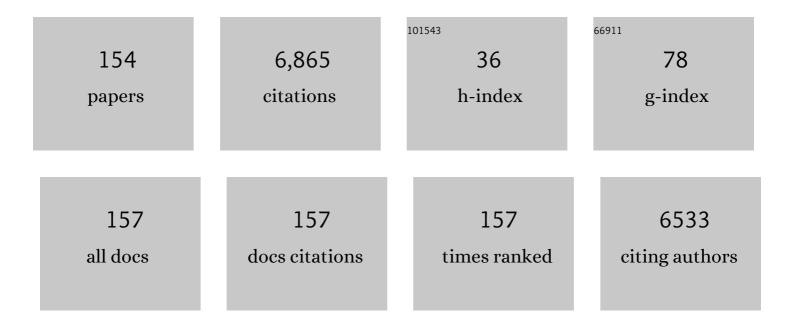
Patrick P Mercier

List of Publications by Year in descending order

Source: https://exaly.com/author-pdf/7893501/publications.pdf Version: 2024-02-01



#	Article	IF	CITATIONS
1	Channel Characterization of Magnetic Human Body Communication. IEEE Transactions on Biomedical Engineering, 2022, 69, 569-579.	4.2	14
2	A Digitally Assisted Multiplexed Neural Recording System With Dynamic Electrode Offset Cancellation via an LMS Interference-Canceling Filter. IEEE Journal of Solid-State Circuits, 2022, 57, 953-964.	5.4	15
3	A GMSK/PAM4 Multichannel Magnetic Human Body Communication Transceiver. IEEE Solid-State Circuits Letters, 2022, 5, 66-69.	2.0	0
4	A 900MHz GFSK and 16-FSK TX Achieving Up to 63.9% TX Efficiency and 76.2% PA Efficiency via a DC-DC-Powered Class-D VCO and a Class-E PA. IEEE Transactions on Circuits and Systems II: Express Briefs, 2022, 69, 3739-3743.	3.0	0
5	An integrated wearable microneedle array for the continuous monitoring of multiple biomarkers in interstitial fluid. Nature Biomedical Engineering, 2022, 6, 1214-1224.	22.5	186
6	A Stochastic Resonance Electrocardiogram Enhancement Algorithm for Robust QRS Detection. IEEE Journal of Biomedical and Health Informatics, 2022, 26, 3743-3754.	6.3	10
7	Analysis and Measurement of Noise Suppression in a Nonlinear Regenerative Amplifier. IEEE Transactions on Circuits and Systems I: Regular Papers, 2022, 69, 4117-4127.	5.4	0
8	An Interference-Resilient BLE-Compatible Wake-Up Receiver Employing Single-Die Multi-Channel FBAR-Based Filtering and a 4-D Wake-Up Signature. IEEE Journal of Solid-State Circuits, 2021, 56, 416-426.	5.4	20
9	A 112-dB SFDR 89-dB SNDR VCO-Based Sensor Front-End Enabled by Background-Calibrated Differential Pulse Code Modulation. IEEE Journal of Solid-State Circuits, 2021, 56, 1046-1057.	5.4	23
10	Low-power integrated circuits for wearable electrophysiology. , 2021, , 163-199.		7
11	A 178.9-dB FoM 128-dB SFDR VCO-Based AFE for ExG Readouts With a Calibration-Free Differential Pulse Code Modulation Technique. IEEE Journal of Solid-State Circuits, 2021, 56, 3236-3246.	5.4	13
12	A 94.2-dB SNDR 142.6-μW VCO-Based Audio ADC With a Split-ADC Differential Pulse Code Modulation Architecture. IEEE Solid-State Circuits Letters, 2021, 4, 121-124.	2.0	7
13	17.5 A 98.2%-Efficiency Reciprocal Direct Charge Recycling Inductor-First DC-DC Converter. , 2021, , .		3
14	A 0.6-mW 16-FSK Receiver Achieving a Sensitivity of â^'103 dBm at 100 kb/s. IEEE Journal of Solid-State Circuits, 2021, 56, 1299-1309.	5.4	11
15	A Dual-Mode Wi-Fi/BLE Wake-Up Receiver. IEEE Journal of Solid-State Circuits, 2021, 56, 1288-1298.	5.4	16
16	A Battery-Connected Inductor-First Flying Capacitor Multilevel Converter Achieving 0.77W/mm ² and 97.1% Peak Efficiency. , 2021, , .		2
17	Maximizing Wireless Power Transfer to Intraocular Implants Under Unconstrained Eye Movements. , 2021, , .		4
18	Investigating well potential parameters on neural spike enhancement in a stochastic-resonance pre-emphasis algorithm. Journal of Neural Engineering, 2021, 18, 046062.	3.5	5

#	Article	IF	CITATIONS
19	A 1.2nW Analog Electrocardiogram Processor Achieving a 99.63% QRS Complex Detection Sensitivity. IEEE Transactions on Biomedical Circuits and Systems, 2021, 15, 617-628.	4.0	11
20	Neural recording and stimulation using wireless networks of microimplants. Nature Electronics, 2021, 4, 604-614.	26.0	81
21	Epidermal Graphene Sensors and Machine Learning for Estimating Swallowed Volume. ACS Applied Nano Materials, 2021, 4, 8126-8134.	5.0	12
22	A Novel Ultrafast Transient Constant on-Time Buck Converter for Multiphase Operation. IEEE Transactions on Power Electronics, 2021, 36, 13096-13106.	7.9	7
23	An Optically Addressed Nanowire-Based Retinal Prosthesis With Wireless Stimulation Waveform Control and Charge Telemetering. IEEE Journal of Solid-State Circuits, 2021, 56, 3263-3273.	5.4	10
24	A 3.75 nW Analog Electrocardiogram Processor Facilitating Stochastic Resonance for Real-Time R-wave Detection. , 2021, , .		4
25	Bell–Bloom Magnetometer Linearization by Intensity Modulation Cancellation. IEEE Transactions on Instrumentation and Measurement, 2020, 69, 883-892.	4.7	5
26	A 22.3-nW, 4.55 cm ² Temperature-Robust Wake-Up Receiver Achieving a Sensitivity of â^69.5 dBm at 9 GHz. IEEE Journal of Solid-State Circuits, 2020, 55, 1530-1541.	5.4	30
27	A Dynamically High-Impedance Charge-Pump-Based LDO With Digital-LDO-Like Properties Achieving a Sub-4-fs FoM. IEEE Journal of Solid-State Circuits, 2020, 55, 719-730.	5.4	26
28	Microneedle-Based Detection of Ketone Bodies along with Glucose and Lactate: Toward Real-Time Continuous Interstitial Fluid Monitoring of Diabetic Ketosis and Ketoacidosis. Analytical Chemistry, 2020, 92, 2291-2300.	6.5	154
29	A Symmetric Modified Multilevel Ladder PMIC for Battery-Connected Applications. IEEE Journal of Solid-State Circuits, 2020, 55, 767-780.	5.4	16
30	A Low-Power Backscatter Modulation System Communicating Across Tens of Meters With Standards-Compliant Wi-Fi Transceivers. IEEE Journal of Solid-State Circuits, 2020, 55, 2959-2969.	5.4	16
31	A â^ 105dB THD 88dB-SNDR VCO-Based Sensor Front-End Enabled by Background-Calibrated Differential Pulse Code Modulation. , 2020, , .		4
32	20.1 A 28ÂμW loT Tag That Can Communicate with Commodity WiFi Transceivers via a Single-Side-Band QPSK Backscatter Communication Technique. , 2020, , .		5
33	A â~'254.1-dB FoM 2.4-GHz Subsampling PLL With a â~'76-dBc Reference Spur by Employing a Varactor-Based Cancellation Technique. IEEE Solid-State Circuits Letters, 2020, 3, 102-105.	2.0	5
34	A Passive-Stacked Third-Order Buck Converter With Inherent Input Filtering Achieving 0.7-W/mm\$^{2}\$ Power Density and 94% Peak Efficiency. IEEE Solid-State Circuits Letters, 2019, 2, 240-243.	2.0	12
35	Power Management for the Internet of Things. , 2019, , .		1
36	A Wearable, Extensible, Open-Source Platform for Hearing Healthcare Research. IEEE Access, 2019, 7, 162083-162101.	4.2	12

#	Article	IF	CITATIONS
37	A Battery-Connected Symmetric Modified Multilevel Ladder Converter Achieving 0.45W/mm2 Power Density and 90% Peak Efficiency. , 2019, , .		2
38	Distributed Microscale Brain Implants with Wireless Power Transfer and Mbps Bi-directional Networked Communications. , 2019, , .		16
39	A Charge-Pump-based Digital LDO Employing an AC-Coupled High-Z Feedback Loop Towards a sub-4fs FoM and a 105,000x Stable Dynamic Current Range. , 2019, , .		6
40	Robust Biopotential Acquisition via a Distributed Multi-Channel FM-ADC. IEEE Transactions on Biomedical Circuits and Systems, 2019, 13, 1229-1242.	4.0	16
41	A Sub-10-pJ/bit 5-Mb/s Magnetic Human Body Communication Transceiver. IEEE Journal of Solid-State Circuits, 2019, 54, 3031-3042.	5.4	25
42	A 763 pW 230 pJ/Conversion Fully Integrated CMOS Temperature-to-Digital Converter With +0.81 °C/â^0.75 °C Inaccuracy. IEEE Journal of Solid-State Circuits, 2019, 54, 2281-2290.	5.4	23
43	17.6 A Sub-40μW 5Mb/s Magnetic Human Body Communication Transceiver Demonstrating Trans-Body Delivery of High-Fidelity Audio to a Wearable In-Ear Headphone. , 2019, , .		7
44	28.2 A 220μW -85dBm Sensitivity BLE-Compliant Wake-up Receiver Achieving -60dB SIR via Single-Die Multi- Channel FBAR-Based Filtering and a 4-Dimentional Wake-Up Signature. , 2019, , .		12
45	22.2 A Rugged Wearable Modular ExG Platform Employing a Distributed Scalable Multi-Channel FM-ADC Achieving 101dB Input Dynamic Range and Motion-Artifact Resilience. , 2019, , .		3
46	8.2 A Continuous-Input-Current Passive-Stacked Third-Order Buck Converter Achieving 0.7W/mm ² Power Density and 94% Peak Efficiency. , 2019, , .		16
47	RF power transmission and its considerations for ECoG implants. , 2019, , 121-144.		0
48	Wireless data communication for ECoG implants. , 2019, , 145-169.		1
49	ECoG signal coding and digitization. , 2019, , 51-71.		0
50	Integrated circuit interfaces for electrocortical stimulation. , 2019, , 73-96.		0
51	Power management for mm-sized ECoG implants. , 2019, , 97-119.		0
52	A 3 mm × 3 mm Fully Integrated Wireless Power Receiver and Neural Interface System-on-Chip. IEEE Transactions on Biomedical Circuits and Systems, 2019, 13, 1736-1746.	4.0	34
53	A Sub-mW 2.4-GHz Active-Mixer-Adopted Sub-Sampling PLL Achieving an FoM of -256 dB. IEEE Journal of Solid-State Circuits, 2019, , 1-11.	5.4	17
54	Introduction to ECoG interfaces. , 2019, , 1-30.		0

#	Article	IF	CITATIONS
55	A Fully Integrated RF-Powered Energy-Replenishing Current-Controlled Stimulator. IEEE Transactions on Biomedical Circuits and Systems, 2019, 13, 191-202.	4.0	18
56	A Fully Integrated Li-Ion-Compatible Hybrid Four-Level DC–DC Converter in 28-nm FDSOI. IEEE Journal of Solid-State Circuits, 2019, 54, 720-732.	5.4	31
57	A 93% Peak Efficiency Fully-Integrated Multilevel Multistate Hybrid DC–DC Converter. IEEE Transactions on Circuits and Systems I: Regular Papers, 2018, 65, 2617-2630.	5.4	23
58	Integrated Coil Design for EV Wireless Charging Systems Using <i>LCC</i> Compensation Topology. IEEE Transactions on Power Electronics, 2018, 33, 9231-9241.	7.9	93
59	A Successive Approximation Recursive Digital Low-Dropout Voltage Regulator With PD Compensation and Sub-LSB Duty Control. IEEE Journal of Solid-State Circuits, 2018, 53, 35-49.	5.4	58
60	A Current-Mode Capacitively-Coupled Chopper Instrumentation Amplifier for Biopotential Recording With Resistive or Capacitive Electrodes. IEEE Transactions on Circuits and Systems II: Express Briefs, 2018, 65, 699-703.	3.0	24
61	A Near-Zero-Power Wake-Up Receiver Achieving â~'69-dBm Sensitivity. IEEE Journal of Solid-State Circuits, 2018, 53, 1640-1652.	5.4	101
62	A Battery-Powered Wireless Ion Sensing System Consuming 5.5 nW of Average Power. IEEE Journal of Solid-State Circuits, 2018, 53, 2043-2053.	5.4	22
63	MISIMO: A multi-input single-inductor multi-output energy harvester employing event-driven MPPT control to achieve 89% peak efficiency and a 60,000x dynamic range in 28nm FDSOI. , 2018, , .		29
64	A sub-1.55mV-accuracy 36.9ps-FOM digital-low-dropout regulator employing switched-capacitor resistance. , 2018, , .		8
65	A 0.3V biofuel-cell-powered glucose/lactate biosensing system employing a 180nW 64dB SNR passive Î'Ï, ADC and a 920MHz wireless transmitter. , 2018, , .		7
66	Design and Analysis of a Three-Phase Wireless Charging System for Lightweight Autonomous Underwater Vehicles. IEEE Transactions on Power Electronics, 2018, 33, 6622-6632.	7.9	162
67	Re-usable electrochemical glucose sensors integrated into a smartphone platform. Biosensors and Bioelectronics, 2018, 101, 181-187.	10.1	93
68	Introduction to the Special Issue on the 2018 IEEE International Solid-State Circuits Conference (ISSCC). IEEE Journal of Solid-State Circuits, 2018, 53, 3015-3016.	5.4	0
69	A 0.01-mm ² Mostly Digital Capacitor-Less AFE for Distributed Autonomous Neural Sensor Nodes. IEEE Solid-State Circuits Letters, 2018, 1, 162-165.	2.0	32
70	AMASS PLL: An Active-Mixer-Adopted Sub-Sampling PLL Achieving an FOM of â^255.5DB and a Reference Spur of â^266.6DBC. , 2018, , .		5
71	A 3.4-pW 0.4-V 469.3 ppm/°C Five-Transistor Current Reference Generator. IEEE Solid-State Circuits Letters, 2018, 1, 122-125.	2.0	33
72	A 0.3-V CMOS Biofuel-Cell-Powered Wireless Glucose/Lactate Biosensing System. IEEE Journal of Solid-State Circuits, 2018, 53, 3126-3139.	5.4	55

#	Article	IF	CITATIONS
73	A 6.1-nW Wake-Up Receiver Achieving â^'80.5-dBm Sensitivity Via a Passive Pseudo-Balun Envelope Detector. IEEE Solid-State Circuits Letters, 2018, 1, 134-137.	2.0	52
74	MISIMO: A Multi-Input Single-Inductor Multi-Output Energy Harvesting Platform in 28-nm FDSOI for Powering Net-Zero-Energy Systems. IEEE Journal of Solid-State Circuits, 2018, 53, 3407-3419.	5.4	74
75	A 0.4-V 0.93-nW/kHz Relaxation Oscillator Exploiting Comparator Temperature-Dependent Delay to Achieve 94-ppm/°C Stability. IEEE Journal of Solid-State Circuits, 2018, 53, 3004-3011.	5.4	47
76	A Rotation-Resilient Wireless Charging System for Lightweight Autonomous Underwater Vehicles. IEEE Transactions on Vehicular Technology, 2018, 67, 6935-6942.	6.3	71
77	A 78%-efficiency li-ion-compatible fully-integrated modified 4-level converter with 0.01–40mW DCM-operation in 28nm FDSOI. , 2018, , .		4
78	A 678-«inline-formula» «tex-math notation="LaTeX">\$mu\$ «/tex-math» «/inline-formula>W Frequency-Modulation-Based ADC With 104-dB Dynamic Range in 44-kHz Bandwidth. IEEE Transactions on Circuits and Systems II: Express Briefs, 2018, 65, 1370-1374.	3.0	6
79	Simultaneous Monitoring of Sweat and Interstitial Fluid Using a Single Wearable Biosensor Platform. Advanced Science, 2018, 5, 1800880.	11.2	371
80	Metallic Nanoislands on Graphene for Monitoring Swallowing Activity in Head and Neck Cancer Patients. ACS Nano, 2018, 12, 5913-5922.	14.6	38
81	Channel Modeling of Miniaturized Battery-Powered Capacitive Human Body Communication Systems. IEEE Transactions on Biomedical Engineering, 2017, 64, 452-462.	4.2	72
82	24.5 A 4.5nW wake-up radio with â^'69dBm sensitivity. , 2017, , .		38
83	20.3 A 100nA-to-2mA successive-approximation digital LDO with PD compensation and sub-LSB duty control achieving a 15.1ns response time at 0.5V. , 2017, , .		33
84	26.4 A 0.4-to-1V 1MHz-to-2GHz switched-capacitor adiabatic clock driver achieving 55.6% clock power reduction. , 2017, , .		5
85	Noise Analysis of Phase-Demodulating Receivers Employing Super-Regenerative Amplification. IEEE Transactions on Microwave Theory and Techniques, 2017, 65, 3299-3311.	4.6	12
86	Eyeglasses based wireless electrolyte and metabolite sensor platform. Lab on A Chip, 2017, 17, 1834-1842.	6.0	211
87	Soft, stretchable, high power density electronic skin-based biofuel cells for scavenging energy from human sweat. Energy and Environmental Science, 2017, 10, 1581-1589.	30.8	309
88	A Recursive Switched-Capacitor House-of-Cards Power Amplifier. IEEE Journal of Solid-State Circuits, 2017, 52, 1719-1738.	5.4	6
89	A three-phase wireless charging system for lightweight autonomous underwater vehicles. , 2017, , .		19
90	A 0.6V 75nW All-CMOS Temperature Sensor With 1.67m°C/mV Supply Sensitivity. IEEE Transactions on Circuits and Systems I: Regular Papers, 2017, 64, 2274-2283.	5.4	34

#	Article	IF	CITATIONS
91	Design of miniaturized wireless power receivers for mm-sized implants. , 2017, , .		13
92	Near-Zero-Power Temperature Sensing via Tunneling Currents Through Complementary Metal-Oxide-Semiconductor Transistors. Scientific Reports, 2017, 7, 4427.	3.3	31
93	Silicon-Integrated High-Density Electrocortical Interfaces. Proceedings of the IEEE, 2017, 105, 11-33.	21.3	68
94	A 420 fW self-regulated 3T voltage reference generator achieving 0.47%/V line regulation from 0.4-to-1.2 V. , 2017, , .		21
95	A 144-MHz Fully Integrated Resonant Regulating Rectifier With Hybrid Pulse Modulation for mm-Sized Implants. IEEE Journal of Solid-State Circuits, 2017, 52, 3043-3055.	5.4	67
96	A 1.6%/V 124.2 pW 9.3 Hz relaxation oscillator featuring a 49.7 pW voltage and current reference generator. , 2017, , .		20
97	A 400 MHz 4.5 nW â^63.8 dBm sensitivity wake-up receiver employing an active pseudo-balun envelope detector. , 2017, , .		28
98	Wireless powering of mm-scale fully-on-chip neural interfaces. , 2017, , .		16
99	A 5.5 nW battery-powered wireless ion sensing system. , 2017, , .		5
100	A 113 pW fully integrated CMOS temperature sensor operating at 0.5 V. , 2017, , .		7
101	The Language of Glove: Wireless gesture decoder with low-power and stretchable hybrid electronics. PLoS ONE, 2017, 12, e0179766.	2.5	55
102	A Reference-Free Capacitive-Discharging Oscillator Architecture Consuming 44.4 pW/75.6 nW at 2.8 Hz/6.4 kHz. IEEE Journal of Solid-State Circuits, 2016, 51, 1423-1435.	5.4	36
103	A multi-channel EEG system featuring single-wire data aggregation via FM-FDM techniques. , 2016, , .		3
104	Flying-Domain DC–DC Power Conversion. IEEE Journal of Solid-State Circuits, 2016, 51, 2830-2842.	5.4	8
105	A 14.5 pW, 31 ppm/°C resistor-less 5 pA current reference employing a self-regulated push-pull voltage reference generator. , 2016, , .		31
106	Noninvasive Alcohol Monitoring Using a Wearable Tattoo-Based Iontophoretic-Biosensing System. ACS Sensors, 2016, 1, 1011-1019.	7.8	460
107	Wearable chemical sensors: Opportunities and challenges. , 2016, , .		15
108	A wearable chemical–electrophysiological hybrid biosensing system for real-time health and fitness monitoring. Nature Communications, 2016, 7, 11650.	12.8	639

#	Article	IF	CITATIONS
109	A fully integrated 144 MHz wireless-power-receiver-on-chip with an adaptive buck-boost regulating rectifier and low-loss H-Tree signal distribution. , 2016, , .		15
110	A recursive house-of-cards digital power amplifier employing a λ/4-less Doherty power combiner in 65nm CMOS. , 2016, , .		1
111	Balloonâ€Embedded Sensors Withstanding Extreme Multiaxial Stretching and Global Bending Mechanical Stress: Towards Environmental and Security Monitoring. Advanced Materials Technologies, 2016, 1, 1600061.	5.8	28
112	12.9 A flying-domain DC-DC converter powering a Cortex-M0 processor with 90.8% efficiency. , 2016, , .		9
113	Narrowband Transmitters: Ultralow-Power Design. IEEE Microwave Magazine, 2015, 16, 130-142.	0.8	6
114	A 1.65 mW PLL-free PSK receiver employing super-regenerative phase sampling. , 2015, , .		8
115	An interdigitated non-contact ECG electrode for impedance compensation and signal restoration. , 2015, , .		5
116	A 51 pW reference-free capacitive-discharging oscillator architecture operating at 2.8 Hz. , 2015, , .		11
117	A single-inductor 7+7 ratio reconfigurable resonant switched-capacitor DC-DC converter with 0.1-to-1.5V output voltage range. , 2015, , .		6
118	A footprint-constrained efficiency roadmap for on-chip switched-capacitor DC-DC converters. , 2015, , .		5
119	Introduction to Ultra Low Power Transceiver Design. Integrated Circuits and Systems, 2015, , 1-23.	0.2	1
120	Architectures for Ultra-Low-Power Multi-Channel Resonator-Based Wireless Transceivers. Integrated Circuits and Systems, 2015, , 97-135.	0.2	0
121	Wireless Power Transfer with Concurrent 200 kHz and 6.78 MHz Operation in a Single Transmitter Device. IEEE Transactions on Power Electronics, 2015, , 1-1.	7.9	68
122	Wearable salivary uric acid mouthguard biosensor with integrated wireless electronics. Biosensors and Bioelectronics, 2015, 74, 1061-1068.	10.1	471
123	A 144MHz integrated resonant regulating rectifier with hybrid pulse modulation. , 2015, , .		9
124	A battery-connected 24-ratio switched capacitor PMIC achieving 95.5%-efficiency. , 2015, , .		29
125	Magnetic human body communication. , 2015, 2015, 1841-4.		20
126	Pulsed Ultra-Wideband Transceivers. Integrated Circuits and Systems, 2015, , 233-280.	0.2	2

#	Article	IF	CITATIONS
127	Guest Editorial—Selected Papers from the 2014 IEEE International Solid-State Circuits Conference. IEEE Transactions on Biomedical Circuits and Systems, 2014, 8, 753-754.	4.0	0
128	A 45-ratio recursively sliced series-parallel switched-capacitor DC-DC converter achieving 86% efficiency. , 2014, , .		13
129	A miniaturized ultrasonic power delivery system. , 2014, , .		10
130	23.2 A 1.1nW energy harvesting system with 544pW quiescent power for next-generation implants. , 2014, , .		25
131	A Recursive Switched-Capacitor DC-DC Converter Achieving <formula formulatype="inline"><tex notation="TeX">\$2^{N}-1\$</tex> Ratios With High Efficiency Over a Wide Output Voltage Range. IEEE Journal of Solid-State Circuits, 2014, 49, 2773-2787.</formula 	5.4	87
132	A 1.1 nW Energy-Harvesting System with 544 pW Quiescent Power for Next-Generation Implants. IEEE Journal of Solid-State Circuits, 2014, 49, 2812-2824.	5.4	131
133	Wearable textile biofuel cells for powering electronics. Journal of Materials Chemistry A, 2014, 2, 18184-18189.	10.3	156
134	A Sub-nW 2.4 GHz Transmitter for Low Data-Rate Sensing Applications. IEEE Journal of Solid-State Circuits, 2014, 49, 1463-1474.	5.4	79
135	Non-invasive mouthguard biosensor for continuous salivary monitoring of metabolites. Analyst, The, 2014, 139, 1632-1636.	3.5	292
136	A 78 pW 1 b/s 2.4 GHz radio transmitter for near-zero-power sensing applications. , 2013, , .		8
137	A 2.4 GHz Multi-Channel FBAR-based Transmitter With an Integrated Pulse-Shaping Power Amplifier. IEEE Journal of Solid-State Circuits, 2013, 48, 1042-1054.	5.4	41
138	Enabling Sub-nW RF circuits through subthreshold leakage management. , 2013, , .		1
139	Rapid Wireless Capacitor Charging Using a Multi-Tapped Inductively-Coupled Secondary Coil. IEEE Transactions on Circuits and Systems I: Regular Papers, 2013, 60, 2263-2272.	5.4	48
140	Guest Editorial—Selected Papers from the 2013 IEEE International Solid-State Circuits Conference (ISSCC). IEEE Transactions on Biomedical Circuits and Systems, 2013, 7, 733-734.	4.0	0
141	Multi-channel 180pJ/b 2.4GHz FBAR-based receiver. , 2012, , .		6
142	A 440pJ/bit 1Mb/s 2.4GHz multi-channel FBAR-based TX and an integrated pulse-shaping PA. , 2012, , .		3
143	Energy extraction from the biologic battery in the inner ear. Nature Biotechnology, 2012, 30, 1240-1243.	17.5	183
144	A Supply-Rail-Coupled eTextiles Transceiver for Body-Area Networks. IEEE Journal of Solid-State Circuits, 2011, 46, 1284-1295.	5.4	12

#	Article	IF	CITATIONS
145	A Pulsed UWB Receiver SoC for Insect Motion Control. IEEE Journal of Solid-State Circuits, 2010, 45, 153-166.	5.4	109
146	A 110µW 10Mb/s etextiles transceiver for body area networks with remote battery power. , 2010, , .		4
147	A Low-Voltage Energy-Sampling IR-UWB Digital Baseband Employing Quadratic Correlation. IEEE Journal of Solid-State Circuits, 2010, 45, 1209-1219.	5.4	24
148	Low-Power Impulse UWB Architectures and Circuits. Proceedings of the IEEE, 2009, 97, 332-352.	21.3	70
149	A pulsed UWB receiver SoC for insect motion control. , 2009, , .		26
150	A 0.55V 16Mb/s 1.6mW non-coherent IR-UWB digital baseband with ±1ns synchronization accuracy. , 2009, , .		13
151	An Energy-Efficient All-Digital UWB Transmitter Employing Dual Capacitively-Coupled Pulse-Shaping Drivers. IEEE Journal of Solid-State Circuits, 2009, 44, 1679-1688.	5.4	112
152	Ultra-low-power UWB for sensor network applications. , 2008, , .		26
153	A 19pJ/pulse UWB transmitter with dual capacitively-coupled digital power amplifiers. , 2008, , .		13
154	Energy Efficient Pulsed-UWB CMOS Circuits and Systems. , 2007, , .		28